Title
Metal-supported solid oxide fuel cells operating with reformed natural gas and sulfur

Journal
International Journal of Hydrogen Energy, 47(21)

ISSN
0360-3199

Authors
Welander, Martha M
Hu, Boxun
Tucker, Michael C

Publication Date
2022-03-01

DOI
10.1016/j.ijhydene.2022.01.170

Peer reviewed

Metal-supported solid oxide fuel cells operating with reformed natural gas and sulfur

Martha M. Welander, Boxun Hu, Michael C. Tucker*

Energy Conversion Group, Lawrence Berkeley National Laboratory, Berkeley, CA 94720

Abstract

The performance, long-term durability, and thermal cycling tolerance of metal supported solid oxide fuel cells (MS-SOFCs) operating with natural gas reformate fuels is assessed. Symmetric MS-SOFCs with composite SDC-Ni anode catalysts and PrO_x cathode catalysts are operated with simulated natural gas steam-reformate and partial-oxidation-reformate fuels with 1 ppm and 5 ppm of sulfur. Cells are operated for 1000 hours with initial degradation rates similar to humidified H_2, and initial performance differences attributed to the lower H_2 concentration in reformate fuels. Additionally, cells tolerate many aggressive thermal cycles with sulfur present, with minimal impact on performance. Post mortem analysis suggests that Ni particle coarsening and Cr deposition are sources of degradation, while carbon and sulfur deposition are not observed. Overall, MS-SOFCs operate successfully with reformed natural gas.

Metal-supported; SOFC; natural gas; sulfur

*mctucker@lbl.gov
Phone 1-510-486-5304
Fax 1-510-486-4260
LBNL; 1 Cyclotron Rd; MS 62-203; Berkely CA 94720; USA

1. Introduction

Fuel flexibility differentiates high temperature solid oxide fuel cells (SOFCs) from their low temperature counterparts such as polymer electrolyte membrane fuel cells (PEMFCs) that must use high-purity H_2 to avoid poisoning the precious metal catalyst. To leverage this fuel flexibility SOFCs need to maintain high performance and durability under operation with a variety of carbon-based fuels such as methane, natural gas (NG), and biogas. As the least carbon intensive fossil fuel with abundant resources, NG has the ability to bridge current and future energy infrastructures. Because SOFCs offer more efficient conversion of NG than is possible by thermoelectric power generation, their operation with NG is of particular interest [1–4].

Symmetric metal supported SOFCs (MS-SOFCs) offer several advantages over state of the art (SoA) anode- or electrolyte-supported SOFCs including: inexpensive materials, rapid start-up capability, increased mechanical strength, and excellent tolerance to thermal and redox cycling [5–9]. MS-SOFCs are well-suited for fast-start portable, mobile, or backup generator applications enabled by their rapid thermal ramp capability [10]. The use of NG for these applications motivates this work. A specific scenario of interest is a residential back-up generator fueled by pipeline NG that can start up quickly in the event of an electric grid shut-down. To keep the system simple and cost-effective, a small battery would provide instantaneous power while the MS-SOFC stack quickly ramps up to operating temperature, NG would be reformed simply with air or water, and minimal or no desulfurization would be used. This requires the MS-SOFC to tolerate carbon and sulfur at typical levels present in pipeline NG during both operation, and heat-up and cool-down ramps.

MS-SOFCs have shown comparable performance to conventional cells (>1 W cm^{-2}) under operation with H_2 [11–14] but only a few studies with carbon-containing fuels have been reported [6,15–18]. MS-SOFCs are subject to similar limitations as SoA cells in hydrocarbon fuels. Ni-based anode catalysts are highly effective at activating C-H bonds and therefore operating conditions must be carefully managed to avoid carbon accumulation or "coking" on the anode surface, which can impede gas transport and block catalytic sites. Approaches to mitigate carbon formation include reforming the hydrocarbon fuel upstream of the fuel cell, and modifying the catalyst composition in the anode [19–22]. A recent report on internal reforming with MS-SOFCs suggest that the performance is inferior to SoA cells and operation with pre-reformed fuels is therefore recommended [17]. As an example, Ceres Power has demonstrated moderate performance and excellent stability over many thousand hours and multiple start-stop cycles with externally steam-reformed fuels [8,16]. Fuel reforming can be categorized according to the oxidizer used in the process [23]. Common reforming processes for NG include steam reforming and partial oxidation (POX). POX reforming involves the partial oxidation of gas with air and can result in simpler systems with advantages for small-scale systems where air and gas can be mixed with a venturi or other simple mixing valve. A main drawback of POX reforming is the dilution of product H_2 with nitrogen. Steam reforming involves the catalytic reaction of fuel with steam to produce H_2. As it requires addition of water, steam reforming leads to somewhat more complicated system. This drawback is offset by production of more H_2 per mole of fuel than POX reforming [24–26].

Carbon based fuels furthermore contain chemical impurities such as sulfur, chlorine, silicon, and phosphorous that impact cell stability. Sulfur compounds are especially notorious for

poisoning the Ni-based anode of SoA SOFCs[27,28]. Experimentally, sulfur is typically introduced into a H_2 fuel stream through the addition of only H_2S [29–31]. This is valid, as the mercaptans and other sulfur compounds contained in NG are transformed into H_2S under SOFC anode conditions [27]. Sulfur poisoning *via* dissociative adsorption of atomic sulfur blocks catalytically active sites, and is largely unavoidable even at low concentrations [27]. Sulfur poisoning studies are almost always performed with H_2 fuel despite awareness that the presence of carbon changes the effects of sulfur [32]. The reforming process is also more sensitive to sulfur than the anode electrochemical reactions [33] and therefore sulfur poisoning during internal reforming of hydrocarbon fuels leads to greater cell degradation. The impact of sulfur-contaminated externally reformed fuel on SOFC anode materials in real electrodes is not well studied, nor is the impact of sulfur on MS-SOFCs.

This work directly assesses the performance, durability, and rapid-startup tolerance of MS-SOFCs operating with reformed pipeline NG fuel containing carbon and sulfur. Specifically, steam reformate and POX reformate with sulfur levels typical of or exceeding pipeline NG have been tested for up to 1000 hours. The steam:carbon and air:carbon ratios of the reformates are chosen to eliminate coking at the operating temperature. The symmetric MS-SOFC design used here offers enhanced mechanical and thermal stability for temperature cycling [34]. Extensive thermal cycling is performed to quantify cell tolerance to carbon and sulfur species under rapidly varying temperatures. The anode is expected to tolerate carbon and sulfur, as it consists primarily of doped ceria and scandia stabilized zirconia which increase ionic conductivity and sulfur oxidation ability [8,35–39]. This work addresses two primary requirements that drive applied research in high temperature energy conversion: cell performance and stability under long term

operation, and resilience of cells toward fuel contamination. To the authors' knowledge, these findings are some of the first to explore the effects of hydrocarbon fuels with sulfur for MS-SOFCs.

2. Material and methods

2.1 Cell fabrication and infiltration

Cells used for this work were symmetric MS-SOFCs consisting of a thin ceramic scandia-ceria-stabilized zirconia (ScSZ) electrolyte (~ 10 μm thick), ScSZ scaffold backbone layers (20 – 30 μm thick) with infiltrated catalysts, and low cost P434L ferritic stainless steel supports (200- 300 μm thick). Button cells were laser cut (Hobby model, Full Spectrum Laser) from laminated green tapes and then debinded in air at 525 °C for 1 h. Cells were sintered at 1350 °C for 2 h in 2% H_2 in Ar and pre-oxidized at 850 °C for 10 h in air to enhance durability. The resulting cells were ~26 mm in diameter (5.3 cm^2 total cell area).

Cell edges were covered with acrylic paint mask (Liquitex), followed by infiltration with metal nitrate catalyst precursor solutions under vacuum. Catalysts were infiltrated into the full area of the porous ScSZ backbones [40]. Infiltration solutions were prepared by mixing stoichiometric amounts of metal nitrates (Sigma Aldrich) with Triton-X 100 (Sigma Aldrich) in water. The anode electrocatalyst was 40 vol% Ni-$Sm_{0.20}Ce_{0.8}0O_{2-\delta}$ ($SDCN_{40}$), followed by 2 cycles of pure Ni infiltration, and the cathode electrode catalyst was Pr_6O_{11} (PrOx). Cells were fired at 800 °C in air for 30 minutes to convert precursors into the appropriate oxide phases. Cathode and anode catalysts were infiltrated 10 times each.

Cell assembly and testing

Platinum wires connected to platinum mesh were spot-welded onto the anode and cathode sides of the cell for electrical connection. Cells were then mounted onto 410 stainless steel rigs and hermetically sealed using 2 layers of glass paste consisting of 80% glass powder GM31107 (Schott) and 20% ink vehicle (Fuel Cell Materials) forming an exposed active cell area of ~ 3 cm^2. Following assembly, test rigs were placed into tube furnaces and heated to 200 °C at 2 °C/min and to 700 °C at 10 °C/min. Cathodes were exposed to static air. Anodes were flushed with N_2 followed by initial reduction in humidified H_2 (3% H_2O). Cells were considered fully reduced when the open circuit voltage stabilized (~1.10V), usually within minutes, and were left at OCV for 1 hour. Once the anode was fully reduced, the catalysts were pre-coarsened for 4 h at 750 °C prior to operation at 700 °C. Simulated NG reformate fuels were custom dry gas mixtures (Praxair) delivered through heated water bubblers and heat-traced lines (Fuel Cell Technologies) to produce the final reformate compositions including H_2O. Reformate compositions at 700 °C were calculated using thermodynamics in Cantera version 2.4, see Supporting Information. Steam-to-carbon and oxygen-to-carbon ratios were selected to prevent coking on the anode surfaces. The steam reformate mixture, representing a fully reformed mixture of 2:1 H_2O:NG, was 62.6% H_2, 16.1% H_2O, 13.6% CO, 5.6% CO_2, 1.6% CH_4 and 0.5% N_2. The partial oxidation (POX) reformate mixture, representing a fully reformed mixture of 3.34:1 air:NG, was 27.6% H_2, 8.6% H_2O, 12.6% CO, 6% CO_2, 0.3% CH_4, and 44.9% N_2. For experiments with sulfur, 75ppm H_2S in H_2 (Praxair) was added to the reformate fuel through a second fuel tube with mixing occurring in the hot zone of the test rig (>650 °C) to avoid sulfur gettering by any carbon deposited in cooler sections of the test rig. For thermal cycling, cells were cooled from 700 °C to <100 °C in 3 to 4 h and quickly re-heated at 40 °C/min to 700 °C. The cooling time and heating ramp rate were limited by the furnace maximum heating and

cooling rates. Total heat-up time averaged 17.5 minutes for all cells. Electrochemical measurements were performed with a VMP3 multi-channel potentiostat and current booster (Biologic). Linear sweep voltammetry (LSV) recorded the I-V polarization curve with a sweep rate of 10 mV/s between voltage limits of 100% and 30% of the measured OCV in order to avoid cell damage at very low voltage. Electrochemical impedance spectroscopy (EIS) measurements were collected with an AC voltage amplitude of 5 mV over a frequency range of 200 kHz to 100 mHz.

2.2 Ex-Situ Analysis

Field emission scanning electron microscope (FESEM) images were collected using a Zeiss Gemini Ultra-55 instrument. An energy dispersive X-ray analysis (EDAX) detector was used for EDS analysis with a beam energy of 20 kV. Raman spectra were collected using a Renishaw inVia Qontor with 488 nm light and 5 acquisitions per scan.

3. Results & Discussion

The performance, durability, and thermal cycling tolerance of MS-SOFCs operating with reformed NG fuels (steam reformate and POX reformate) were assessed. Both types of fuels were tested under various operating conditions including galvanostatic hold at 700 °C, thermal cycling between < 100 °C and 700 °C, and performance assessment with 5 ppm and 1 ppm of H_2S. Operating conditions were carefully chosen to maximize performance and avoid carbon deposition by choosing steam:carbon and air:carbon ratios that are a small margin outside of the thermodynamically favorable regions for carbon formation.

Compared to baseline performance with H_2 fuel, performance with sulfur-free reformate fuels was lower. This lower performance is a result of hydrogen dilution and increased partial pressure of oxygen accompanying oxidized species (CO_2, H_2O) in the reformates. These features are apparent in the reduced OCV and increased concentration polarization seen in Figure 1a. The mass transport limitation observed in the polarization curves below ~0.5 V is especially pronounced for POX reformate due to the low hydrogen concentration (27.6% H_2 in POX reformate vs. 62.6 % H_2 in steam reformate). Peak power density was ~0.1 Wcm^{-2} lower for POX reformate than steam reformate because POX produces less H_2 per mole of fuel than steam reforming [26] and electrochemical oxidation of H_2 is kinetically preferred over CO [41,42]. Despite differences in initial performance, durability over 200 h was similar for all fuel types, Figure 1b. Current density dropped 35 to 40% with the majority of the degradation consistently occurring in the first 100 h. Due to low Ni loading [43], catalyst coarsening during the break in period (~100 h) is expected to reduce performance [44]. Because steam-to-carbon and air-to-carbon ratios were chosen outside of the thermodynamic coking regions, carbon-containing species in the fuel did not accelerate degradation under operation with reformates.

Figure 1. Performance with reformate fuels at 700 °C. (a) Baseline polarization curves and (b) initial durability of cells operating with 100 sccm H_2, steam refromate (SR), or POX reformate at 0.75 V.

The MS-SOFCs tolerate sulfur content representative of pipeline NG. Addition of 1 ppm and 5 ppm of sulfur minimally impact the initial performance with reformate fuels, Figure 2.

These sulfur levels in the reformed fuels represent 5 ppm (typical) and 18 ppm (abnormally high) sulfur, respectively, in the NG pipeline and exceed typical sulfur-tolerance levels, ~1 ppm, of ceramic SoA SOFCs [38,45,46].The pipeline sulfur is significantly diluted as the reforming reactions create additional moles of gas, for example complete oxidation of 1 mole of methane yields 3 moles of carbon dioxide and water. There is minimal difference in the performance with no sulfur and 1 ppm sulfur. A moderate performance drop was observed for addition of 5 ppm sulfur. The addition of sulfur does not significantly impact short-term durability, Figure 3. The small Ni particle size and intimate mixing between Ni and SDC in the infiltrated MS-SOFC anode, and oxidation during polarization[27,38] are thought to enable the high sulfur tolerance. Additionally, Ni particles in the metal support may getter S without impacting performance, as the stainless steel, not the Ni, acts as the electrical conductor.

Figure 2. Performance with reformate fuels and sulfur. Baseline polarization curves of cells operating with (a) steam reformate (SR), and (b) POX reformate with no sulfur present in fuel stream, 1 ppm sulfur present in fuel stream, and 5 ppm sulfur present in fuel stream at 700 °C.

Figure 3. Cell degradation behaviour with and without sulfur. Degradation with (a) steam reformate and (b) POX reformate with 0, 1, and 5 ppm sulfur at 0.75 V and 700 °C.

MS-SOFCs were found to tolerate rapid thermal cycling under reformate fuels with 5 ppm sulfur. The presence of carbon and sulfur species did not accelerate cell degradation relative

to previous thermal cycling work with H_2 [47]. This is a significant finding, as the presence of sulfur is known to damage Ni in SoA cells during cooling *via* formation of a low-melting Ni-S phase[48,49] . We presume the tolerance observed here is due to the low Ni content, small Ni particle size, and intimate mixing with ceria. While some solid carbon was thermodynamically expected at lower temperatures during thermal cycling this was possibly kinetically limited, see Supporting Information. Repeated thermal cycling with rapid heat-up (17.5 min) was done with steam and POX reformate with 5 ppm sulfur for 40 and 25 thermal cycles respectively, Figure 4. The cells tolerate this aggressive thermal cycling, with only moderate irreversible degradation part of which is attributed to hold time at operating temperature. Peak power density for steam reformate dropped 11% between the first and 40th thermal cycle with less than 0.02 W cm^{-2} difference at the expected operating voltage of 0.75 V. Peak power density for POX reformate dropped 12% between the first and 25th thermal cycle with no change observed at 0.75 V. Under both fuels, the majority of the performance decline was observed in the first 10 thermal cycles and can be attributed to break in, similar to the rapid degradation observed in the first 24 h of potentiostatic operation, Figure 3. The OCVs do not change, confirming that the cells and seals are mechanically robust towards thermal cycling. Cell impedance was characterized with EIS before and after thermal cycling. For steam reformate the polarization resistance increases by 0.4 Ω cm^2 and a small increase in ohmic impedance occurs, Figure 4c. For POX reformate the high-frequency polarization arc is slightly elongated after cycling and noise in the low frequency region obscures any changes, Figure 4f. The negligible change in ohmic impedance confirms that connectivity between the electrolyte, electrode, and support layers remains intact after thermal cycling.

Figure 4. Thermal cycling of reformate fuels with 5 ppm sulfur. (a-c) Steam reformate with 5 ppm sulfur and (d-f) POX reformate with 5 ppm sulfur. (a,d) OCV and peak power density during thermal cycling. Initial and final (b, e) polarization curves and (c,f) EIS spectra at 700 °C.

Cells operated successfully for 1000 h with steam and POX reformates containing 1 ppm sulfur, Figure 5. The majority of degradation occurred in the first 200 h, after which the degradation rate stabilized. For steam reformate, degradation was 60% over 1000 h, with 32% occurring in the first 100 h and 8% in the last 500 h, Figure 5a-d. The degradation rate was 44%/kh for the last 500 h. For POX reformate, degradation was 54% over 1000 h, with 25% occurring in the first 100 h and 14% in the last 500 h, Figure 5e-h. The degradation rate was 36%/kh for the last 500 h. Performance was monitored regularly by LSV and EIS measurements at OCV. Polarization curves for both fuels evolve rapidly in the first 300 h, transitioning from a convex polarization curve with significant concentration polarization at high current density to more linear polarization behavior. Both ohmic and polarization resistances increased for both fuels, Fig 5(c, g). For steam reformate, ohmic resistance increased 0.29 Ω cm^2 and polarization resistance increased 0.75 Ω cm^2. For POX reformate, ohmic resistance increased by 0.27 Ω cm^2 and polarization resistance by 0.48 Ω cm^2. While ohmic resistance increased in both cases, the polarization resistance increase is significantly larger. This suggests degradation is dominated by electrode reactions rather than electrolyte structure or composition evolution, and is consistent with previous work that correlates increased polarization resistance with catalyst coarsening [6]. Increased ohmic resistance is likely due to catalyst structure evolution including Ni agglomeration (Figure 6b), and decreased conductivity as a result of Cr reaction with the cathode

catalyst [50]. A small change in the OCV at the end of steam reformate operation likely arises from damage to the seal, or possibly an electrolyte pinhole.

Figure 5. Long term operation with reformate fuels and 1 ppm sulfur at 700 °C. (a-d) Steam reformate and (e-h) POX reformate with 1 ppm sulfur. (a, e) Potentiostatic operation for approximately 1000 h at 0.75 V. Initial, intermediate, and final (b, f) polarization curves and (c, g) EIS spectra. (d, h) Quantified OCV, peak power density, ohmic impedance, and polarization impedance.

Post mortem analysis confirmed Ni coarsening at the anode to be the primary degradation mode during 1000 h tests. Catalyst particle coarsening was observed from FE-SEM images collected inside the catalyst-coated pores of the active electrodes. The anode and cathode catalyst structures after 1000 h testing with steam reformate were compared to a fresh cell that was held at OCV for 2 h with H_2 fuel to reduce the anode catalyst, Figure 6. Severe Ni particle coarsening was observed on the anode after 1000 h. Individual Ni particles up to ~0.5 μm in diameter evolved from the dispersed submicron-scale catalyst network. This particle coarsening is consistent with the increased EIS polarization impedance discussed above. Compared to previous long-term testing of MS-SOFCs, these Ni particles are dramatically larger [47,51]. The increased size can in part be attributed to additional pure-Ni infiltration cycles used for this work. While the role of steam content, sulfur, and carbon species on coarsening should be investigated in more detail, previous work suggests that sulfur can impact the percolation of Ni particles at high overpotentials [52]. More pronounced cathode catalyst particles were observed after 1000 h operation although significant cathode coarsening did not occur. Compared to the anode particle

coarsening, cathode evolution was much less severe and its contribution to cell degradation is therefore considered to be minor. Similar degradation modes were observed after 1000 h testing in POX reformate.

Figure 6. Evolution of catalyst nano-structure upon long-term operation. FE-SEM images of (a, b) anode and (c, d) cathode after (a, c) 2 h at OCV or (b, d) 1000 h operation with steam reformate with 1 ppm sulfur.

EDS mapping of the cathode after 1000 h steam reformate operation confirmed that some chromium poisoning of the praseodymium oxide catalyst occurred. This phenomenon has been studied in detail previously and contributes to cell degradation for both MS-SOFCs and anode-supported SOFCs with chromium-containing stainless steel interconnects [51,53]. The atomic ratio of Cr to Pr observed at several sites in the cathode active area was in the range of 4 to 10 at %, far below that seen in previous studies [37, 39]. The rapid, high temperature infiltration procedure used in this study is thought to result in a denser, lower surface area catalyst coating on the stainless steel which blocks Cr evaporation and may explain this relatively mild Cr poisoning. Cr poisoning of the Pr catalyst is therefore considered a secondary degradation mechanism in this study.

Sulfur and carbon deposition were not detected on the anodes after 1000 h of reformate operation. With EDS, sulfur was not observed and the small carbon background signal was similar to that normally observed on MS-SOFCs operated with hydrogen, Figure 7a [51]. Lack of sulfur adsorption detection could be explained by instrument detection limits [48] and the

relatively low sulfur concentration used. Carbon deposition was not thermodynamically predicted, and its absence was confirmed using ex-situ Raman analysis, Figure 7b. The anode surface showed clear signals from zirconia species but no indication of the carbon bands typically observed as a result of coking such as highly ordered graphite at ~1560 cm^{-1} or disordered graphite at 1350 cm^{-1}. The lack of spectroscopically observable carbon ex-situ after flushing the anode chamber with hydrogen and cooling down, however, does not exclude possible carbon accumulation during operation [54].

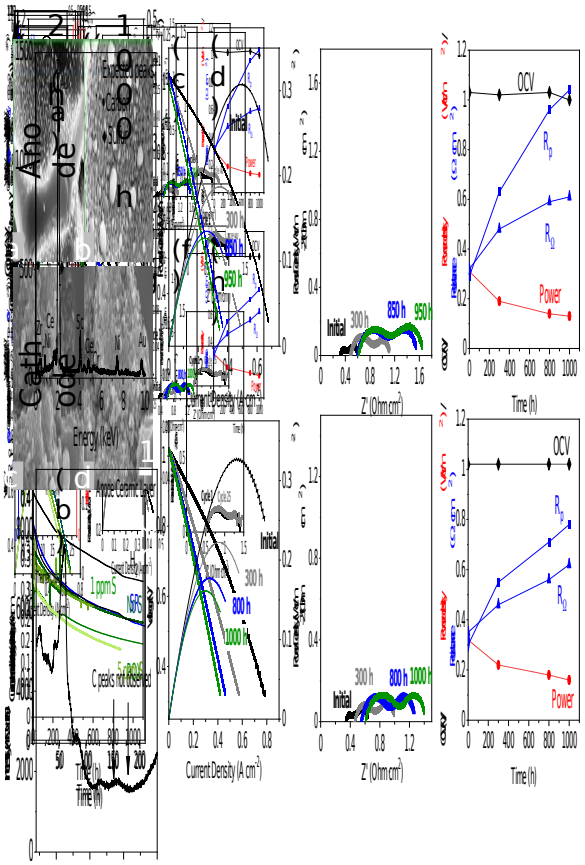

Figure 7. Post mortem analysis of sulfur and carbon deposition. Representative post mortem EDS and Raman analysis of ceramic anode layer. No evidence of sulfur or carbon adsorption is observed.

4. Conclusion

MS-SOFCs successfully operate with steam reformate and POX reformate fuel, with sulfur levels relevant to pipeline NG. Cells were able to withstand repeated thermal cycles and 1000 h of operation. Post mortem analysis suggests that carbon accumulation did not occur on cell anodes under the chosen operating conditions, as expected from thermodynamics. Addition of 1 ppm sulfur does not impact performance. Addition of 5 ppm sulfur moderately reduces initial performance, but EDS analysis showed no evidence of sulfur accumulation post mortem. Irreversible degradation occurring during 1000 h operation arises primarily from significant Ni particle coarsening. Slight Cr poisoning of the cathode catalyst was also observed. This work demonstrates the utility of MS-SOFCs for rapid-startup applications with NG fuel containing sulfur.

Acknowledgements

We thank Jeff Chase and Matthias Riegraf for helpful discussion and Rohit Satish and Robert Kostecki for help collecting Raman data. This work was funded by the Southern California Gas Company (SoCalGas), a public utility company. This work was funded in part by the U.S. Department of Energy under contract no. DE-AC02-05CH11231. Work at the Molecular Foundry was supported by the Office of Science, Office of Basic Energy Sciences, of the U.S. Department of Energy under Contract No. DE-AC02-05CH11231. The views and opinions of the authors expressed herein do not necessarily state or reflect those of the United States Government or any agency thereof. Neither the United States Government nor any agency

thereof, nor any of their employees, makes any warranty, expressed or implied, or assumes any legal liability or responsibility for the accuracy, completeness, or usefulness of any information, apparatus, product, or process disclosed, or represents that its use would not infringe privately owned rights.

References

[1] M. Boder, R. Dittmeyer, Catalytic modification of conventional SOFC anodes with a view to reducing their activity for direct internal reforming of natural gas, J. Power Sources. 155 (2006) 13–22. https://doi.org/10.1016/j.jpowsour.2004.11.075.

[2] T.M. Gür, Comprehensive review of methane conversion in solid oxide fuel cells: Prospects for efficient electricity generation from natural gas, Prog. Energy Combust. Sci. 54 (2016) 1–64. https://doi.org/10.1016/j.pecs.2015.10.004.

[3] R. Scaccabarozzi, M. Gatti, S. Campanari, E. Martelli, Solid oxide semi-closed CO2 cycle: A hybrid power cycle with 75% net efficiency and zero emissions, Appl. Energy. 290 (2021) 116711. https://doi.org/10.1016/j.apenergy.2021.116711.

[4] J. Zhou, Z. Wang, M. Han, Z. Sun, K. Sun, Optimization of a 30 kW SOFC combined heat and power system with different cycles and hydrocarbon fuels, Int. J. Hydrog. Energy. 47 (2022) 4109–4119. https://doi.org/10.1016/j.ijhydene.2021.11.049.

[5] D. Udomsilp, J. Rechberger, R. Neubauer, C. Bischof, F. Thaler, W. Schafbauer, N.H. Menzler, L.G.J. de Haart, A. Nenning, A.K. Opitz, O. Guillon, M. Bram, Metal-Supported Solid Oxide Fuel Cells with Exceptionally High Power Density for Range Extender Systems, Cell Rep. Phys. Sci. 1 (2020) 100072. https://doi.org/10.1016/j.xcrp.2020.100072.

[6] E. Dogdibegovic, Y. Fukuyama, M.C. Tucker, Ethanol internal reforming in solid oxide fuel cells: A path toward high performance metal-supported cells for vehicular applications, J. Power Sources. 449 (2020) 227598. https://doi.org/10.1016/j.jpowsour.2019.227598.

[7] A. Hagen, X. Sun, B.R. Sudireddy, \AA H. Persson, Metal Supported SOFCs for Mobile Applications using Hydrocarbon Fuels, J. Electrochem. Soc. 167 (2020) 104510. https://doi.org/10.1149/1945-7111/ab9b9d.

[8] R.T. Leah, A. Bone, A. Selcuk, M. Rahman, A. Clare, M. Lankin, F. Felix, S. Mukerjee, M. Selby, Latest Results and Commercialization of the Ceres Power SteelCell® Technology Platform, ECS Trans. 91 (2019) 51–61. https://doi.org/10.1149/09101.0051ecst.

[9] M.C. Tucker, Progress in metal-supported solid oxide fuel cells: A review, J. Power Sources. 195 (2010) 4570–4582. https://doi.org/10.1016/j.jpowsour.2010.02.035.

[10] Y. Matus, L. Dejonghe, C. Jacobson, S. Visco, Metal-supported solid oxide fuel cell membranes for rapid thermal cycling, Solid State Ion. 176 (2005) 443–449. https://doi.org/10.1016/j.ssi.2004.09.056.

[11] P. Blennow, J. Hjelm, T. Klemensø, A. Persson, K. Brodersen, A. Srivastava, H. Frandsen, M. Lundberg, S. Ramousse, M. Mogensen, Development of Planar Metal Supported SOFC with Novel Cermet Anode, ECS Trans. 25 (2019) 701–710. https://doi.org/10.1149/1.3205585.
[12] T. Klemensø, J. Nielsen, P. Blennow, A. Persson, T. Stegk, P. Hjalmarsson, B. Christensen, S. Sønderby, J. Hjelm, S. Ramousse, Development of Long-Term Stable and High-Performing Metal-Supported SOFCs, ECS Trans. 35 (2019) 369–378. https://doi.org/10.1149/1.3570011.
[13] M.C. Tucker, Development of High Power Density Metal-Supported Solid Oxide Fuel Cells, Energy Technol. 5 (2017) 2175–2181. https://doi.org/10.1002/ente.201700242.
[14] J. Nielsen, Å.H. Persson, T.T. Muhl, K. Brodersen, Towards High Power Density Metal Supported Solid Oxide Fuel Cell for Mobile Applications, J. Electrochem. Soc. 165 (2018) F90–F96. https://doi.org/10.1149/2.0741802jes.
[15] A. Hagen, X. Sun, B.R. Sudireddy, A.H. Persson, Internal Reforming on Metal Supported SOFCs, ECS Trans. 91 (2019) 867–876. https://doi.org/10.1149/09101.0867ecst.
[16] R.T. Leah, A. Bone, M. Lankin, A. Selcuk, M. Rahman, A. Clare, L. Rees, S. Phillip, S. Mukerjee, M. Selby, Ceres Power Steel Cell Technology: Rapid Progress Towards a Truly Commercially Viable SOFC, ECS Trans. 68 (2015) 95–107. https://doi.org/10.1149/06801.0095ecst.
[17] J.O. Christensen, A. Hagen, B.R. Sudireddy, Performance of Metal Supported SOFCs Operated in Hydrocarbon Fuels and at Low (<650˚C) Temperatures, ECS Trans. 103 (2021) 713–724. https://doi.org/10.1149/10301.0713ecst.
[18] M. Dewa, W. Yu, N. Dale, A.M. Hussain, M.G. Norton, S. Ha, Recent progress in integration of reforming catalyst on metal-supported SOFC for hydrocarbon and logistic fuels, Int. J. Hydrog. Energy. 46 (2021) 33523–33540. https://doi.org/10.1016/j.ijhydene.2021.07.177.
[19] G.J. Offer, J. Mermelstein, E. Brightman, N.P. Brandon, Thermodynamics and Kinetics of the Interaction of Carbon and Sulfur with Solid Oxide fuel Cell Anodes, J. Am. Ceram. Soc. 92 (2009) 763–780. https://doi.org/10.1111/j.1551-2916.2009.02980.x.
[20] H. He, J.M. Hill, Carbon deposition on Ni/YSZ composites exposed to humidified methane, Appl. Catal. Gen. 317 (2007) 284–292. https://doi.org/10.1016/j.apcata.2006.10.040.
[21] Z. Tao, G. Hou, N. Xu, Q. Zhang, A highly coking-resistant solid oxide fuel cell with a nickel doped ceria: Ce1−xNixO2−y reformation layer, Int. J. Hydrog. Energy. 39 (2014) 5113–5120. https://doi.org/10.1016/j.ijhydene.2014.01.092.
[22] H. Li, Y. Tian, Z. Wang, F. Qie, Y. Li, An all perovskite direct methanol solid oxide fuel cell with high resistance to carbon formation at the anode, RSC Adv. 2 (2012) 3857–3863. https://doi.org/10.1039/C2RA01256A.
[23] J. Bae, Chapter 8 - Fuel Processor Lifetime and Reliability in Solid Oxide Fuel Cells, in: N.P. Brandon, E. Ruiz-Trejo, P. Boldrin (Eds.), Solid Oxide Fuel Cell Lifetime Reliab., Academic Press, 2017: pp. 145–171. https://doi.org/10.1016/B978-0-08-101102-7.00008-8.
[24] Y.M.A. Welaya, M.M. El Gohary, N.R. Ammar, Steam and partial oxidation reforming options for hydrogen production from fossil fuels for PEM fuel cells, Alex. Eng. J. 51 (2012) 69–75. https://doi.org/10.1016/j.aej.2012.03.001.

[25] J. Reinkingh, M. Petch, Mixed POX/steam-reforming reactor design considerations, in: Handb. Fuel Cells, American Cancer Society, 2010. https://doi.org/10.1002/9780470974001.f302014.
[26] A. Fuente Cuesta, C. Savaniu, K.D. Pointon, J.T.S. Irvine, 'Waste-to-Energy' Fuel Cell Systems, ECS Trans. 91 (2019) 1581–1590. https://doi.org/10.1149/09101.1581ecst.
[27] P. Boldrin, E. Ruiz-Trejo, J. Mermelstein, J.M. Bermúdez Menéndez, T. Ramírez Reina, N.P. Brandon, Strategies for Carbon and Sulfur Tolerant Solid Oxide Fuel Cell Materials, Incorporating Lessons from Heterogeneous Catalysis, Chem. Rev. 116 (2016) 13633–13684. https://doi.org/10.1021/acs.chemrev.6b00284.
[28] A. Weber, S. Dierickx, A. Kromp, E. Ivers-Tiffée, Sulfur Poisoning of Anode-Supported SOFCs under Reformate Operation, Fuel Cells. 13 (2013) 487–493. https://doi.org/10.1002/fuce.201200180.
[29] J.F.B. Rasmussen, A. Hagen, The effect of H2S on the performance of Ni–YSZ anodes in solid oxide fuel cells, J. Power Sources. 191 (2009) 534–541. https://doi.org/10.1016/j.jpowsour.2009.02.001.
[30] K. Sasaki, K. Haga, T. Yoshizumi, D. Minematsu, E. Yuki, R. Liu, C. Uryu, T. Oshima, T. Ogura, Y. Shiratori, K. Ito, M. Koyama, K. Yokomoto, Chemical durability of Solid Oxide Fuel Cells: Influence of impurities on long-term performance, J. Power Sources. 196 (2011) 9130–9140. https://doi.org/10.1016/j.jpowsour.2010.09.122.
[31] P. Steiger, D. Burnat, H. Madi, A. Mai, L. Holzer, J. Van Herle, O. Kröcher, A. Heel, D. Ferri, Sulfur Poisoning Recovery on a Solid Oxide Fuel Cell Anode Material through Reversible Segregation of Nickel, Chem. Mater. 31 (2019) 748–758. https://doi.org/10.1021/acs.chemmater.8b03669.
[32] P. Boldrin, N.P. Brandon, Progress and outlook for solid oxide fuel cells for transportation applications, Nat. Catal. 2 (2019) 571–577. https://doi.org/10.1038/s41929-019-0310-y.
[33] H. Langnickel, A. Hagen, New Methodology of Studying H_2S Poisoning Effects on SOFC's Fueled by Carbon Containing Fuels like Biogas, ECS Trans. 91 (2019) 511–521. https://doi.org/10.1149/09101.0511ecst.
[34] M.C. Tucker, A.S. Ying, Metal-supported solid oxide fuel cells operated in direct-flame configuration, Int. J. Hydrog. Energy. 42 (2017) 24426–24434. https://doi.org/10.1016/j.ijhydene.2017.07.224.
[35] D. Knapp, T. Ziegler, Methane Dissociation on the Ceria (111) Surface, J. Phys. Chem. C. 112 (2008) 17311–17318. https://doi.org/10.1021/jp8039862.
[36] M. Shishkin, T. Ziegler, Coke-Tolerant Ni/BaCe1–xYxO3−δ Anodes for Solid Oxide Fuel Cells: DFT+U Study, J. Phys. Chem. C. 117 (2013) 7086–7096. https://doi.org/10.1021/jp312485q.
[37] Y. Lin, Z. Zhan, S.A. Barnett, Improving the stability of direct-methane solid oxide fuel cells using anode barrier layers, J. Power Sources. 158 (2006) 1313–1316. https://doi.org/10.1016/j.jpowsour.2005.09.060.
[38] H. Kurokawa, T.Z. Sholklapper, C.P. Jacobson, L.C.D. Jonghe, S.J. Visco, Ceria Nanocoating for Sulfur Tolerant Ni-Based Anodes of Solid Oxide Fuel Cells, Electrochem. Solid-State Lett. 10 (2007) B135. https://doi.org/10.1149/1.2748630.
[39] A. Trovarelli, C. de Leitenburg, M. Boaro, G. Dolcetti, The utilization of ceria in industrial catalysis, Catal. Today. 50 (1999) 353–367. https://doi.org/10.1016/S0920-5861(98)00515-X.

[40] E. Dogdibegovic, Y. Cheng, F. Shen, R. Wang, B. Hu, M.C. Tucker, Scaleup and manufacturability of symmetric-structured metal-supported solid oxide fuel cells, J. Power Sources. 489 (2021) 229439. https://doi.org/10.1016/j.jpowsour.2020.229439.
[41] W.A. Maza, E.D. Pomeroy, D.A. Steinhurst, R.A. Walker, J.C. Owrutsky, Operando optical studies of sulfur contamination in syngas operation of solid oxide fuel cells, J. Power Sources. 510 (2021) 230398. https://doi.org/10.1016/j.jpowsour.2021.230398.
[42] H.C. Patel, A.N. Tabish, F. Comelli, P.V. Aravind, Oxidation of H2, CO and syngas mixtures on ceria and nickel pattern anodes, Appl. Energy. 154 (2015) 912–920. https://doi.org/10.1016/j.apenergy.2015.05.049.
[43] M.C. Tucker, G.Y. Lau, C.P. Jacobson, L.C. DeJonghe, S.J. Visco, Performance of metal-supported SOFCs with infiltrated electrodes, J. Power Sources. 171 (2007) 477–482. https://doi.org/10.1016/j.jpowsour.2007.06.076.
[44] E. Dogdibegovic, R. Wang, G.Y. Lau, A. Karimaghaloo, M.H. Lee, M.C. Tucker, Progress in durability of metal-supported solid oxide fuel cells with infiltrated electrodes, J. Power Sources. 437 (2019) 226935. https://doi.org/10.1016/j.jpowsour.2019.226935.
[45] N. Mahato, A. Banerjee, A. Gupta, S. Omar, K. Balani, Progress in material selection for solid oxide fuel cell technology: A review, Prog. Mater. Sci. 72 (2015) 141–337. https://doi.org/10.1016/j.pmatsci.2015.01.001.
[46] Z. Cheng, J.-H. Wang, Y. Choi, L. Yang, M.C. Lin, M. Liu, From Ni-YSZ to sulfur-tolerant anode materials for SOFCs: electrochemical behavior, in situ characterization, modeling, and future perspectives, Energy Environ. Sci. 4 (2011) 4380–4409. https://doi.org/10.1039/C1EE01758F.
[47] M.C. Tucker, Durability of symmetric-structured metal-supported solid oxide fuel cells, J. Power Sources. 369 (2017) 6–12. https://doi.org/10.1016/j.jpowsour.2017.09.075.
[48] J.H. Kim, M. Liu, Y. Chen, R. Murphy, Y. Choi, Y. Liu, M. Liu, Understanding the Impact of Sulfur Poisoning on the Methane-Reforming Activity of a Solid Oxide Fuel Cell Anode, ACS Catal. (2021) 13556–13566. https://doi.org/10.1021/acscatal.1c02470.
[49] H. Okamoto, Ni-S (Nickel-Sulfur), J. Phase Equilibria Diffus. 30 (2009) 123–123. https://doi.org/10.1007/s11669-008-9430-9.
[50] G.Y. Lau, M.C. Tucker, C.P. Jacobson, S.J. Visco, S.H. Gleixner, L.C. DeJonghe, Chromium transport by solid state diffusion on solid oxide fuel cell cathode, J. Power Sources. 195 (2010) 7540–7547. https://doi.org/10.1016/j.jpowsour.2010.06.017.
[51] F. Shen, R. Wang, M.C. Tucker, Long term durability test and post mortem for metal-supported solid oxide electrolysis cells, J. Power Sources. 474 (2020) 228618. https://doi.org/10.1016/j.jpowsour.2020.228618.
[52] A. Hauch, A. Hagen, J. Hjelm, T. Ramos, Sulfur Poisoning of SOFC Anodes: Effect of Overpotential on Long-Term Degradation, J. Electrochem. Soc. 161 (2014) F734. https://doi.org/10.1149/2.080406jes.
[53] S.C. Paulson, V.I. Birss, Chromium poisoning of LSM-YSZ SOFC catho des I. detailed study of the distribution of chromium species at a porous, single-phase cathode, J. Electrochem. Soc. 151 (2004) A1961–A1968. https://doi.org/10.1149/1.1806392.
[54] M.M. Welander, D.B. Drasbæk, M.L. Traulsen, B.R. Sudireddy, P. Holtappels, R.A. Walker, What does carbon tolerant really mean? Operando vibrational

studies of carbon accumulation on novel solid oxide fuel cell anodes prepared by infiltration, Phys. Chem. Chem. Phys. 22 (2020) 9815–9823. https://doi.org/10.1039/D0CP00195C.